

Review Article

Cerenkov imaging - a new modality for molecular imaging

Daniel LJ Thorek¹, Robbie Robertson², Wassifa A Bacchus³, Jaeseung Hahn³, Julie Rothberg⁴, Bradley J Beattie⁵, Jan Grimm^{1,4}

¹Department of Radiology, Memorial Sloan-Kettering Cancer Center, New York, New York; ²Millennium Pharmaceuticals, The Takeda Company, Biomedical Imaging Group, Cambridge, Massachusetts; ³Department of Biomedical Engineering, City College of New York, City University of New York, 160 Convent Avenue, New York, New York; ⁴Program in Molecular Pharmacology and Chemistry, Memorial Sloan-Kettering Cancer Center, New York, New York; ⁵Medical Physics, Memorial Sloan-Kettering Cancer Center, 1275 York Avenue, New York, NY 10065, USA

Received January 29, 2012; accepted February 25, 2012; Epub March 28, 2012; Published April 15, 2012

Abstract: Cerenkov luminescence imaging (CLI) is an emerging hybrid modality that utilizes the light emission from many commonly used medical isotopes. Cerenkov radiation (CR) is produced when charged particles travel through a dielectric medium faster than the speed of light in that medium. First described in detail nearly 100 years ago, CR has only recently applied for biomedical imaging purposes. The modality is of considerable interest as it enables the use of widespread luminescence imaging equipment to visualize clinical diagnostic (all PET radioisotopes) and many therapeutic radionuclides. The amount of light detected in CLI applications is significantly lower than other that in other optical imaging techniques such as bioluminescence and fluorescence. However, significant advantages include the use of approved radiotracers and lack of an incident light source, resulting in high signal to background ratios. As well, multiple subjects may be imaged concurrently (up to 5 in common bioluminescent equipment), conferring both cost and time benefits. This review summarizes the field of Cerenkov luminescence imaging to date. Applications of CLI discussed include intraoperative radionuclide-guided surgery, monitoring of therapeutic efficacy, tomographic optical imaging capabilities, and the ability to perform multiplexed imaging using fluorophores excited by the Cerenkov radiation. While technical challenges still exist, Cerenkov imaging has materialized as an important molecular imaging modality.

Keywords: Cerenkov radiation, PET, optical imaging, fluorescence

Introduction

Nuclear imaging techniques are essential tools of disease imaging and scientific study in the clinical and research settings. Techniques including Positron Emission Tomography (PET), Single Photon Emission Computed Tomography (SPECT) and autoradiography provide researchers with extremely sensitive visualization of injected tracers throughout an organism or biological specimen. A recent development in the field of radioisotope imaging has been the ability to visualize a decay signal of a radioisotope utilizing a cooled and highly sensitive CCD camera. This optical decay signal is Cerenkov Radiation (CR); the visible wavelength light produced by a charged particle travelling through a dielectric medium faster than the speed of light in that medium [1].

The Cerenkov optical phenomenon has been utilized since the 1940's for photomultiplier tube scintillation counting [2, 3], detection of subatomic particles for physical and astronomical studies and the estimation of fuel rod activity in nuclear power plants. However, considerable interest has been generated following demonstration of the imaging of this light using bioluminescence imaging equipment, *in vivo* [4]. Optical imaging techniques pair high resolution and sensitivity to provide a fundamental resource for preclinical biomedical research.

Cerenkov radiation

The first observation of CR is believed to be an account from Dr. Curie over a century ago [5]. Pavel A. Cerenkov later characterized the phenomenon, which earned him a share of the

Cerenkov luminescence imaging

1958 Physics Nobel Prize together with Ilya Frank and Igor Tamm. The radiation is polarized and continuous with an intensity distribution that is inversely proportional to the square of the wavelength. Thus, the majority of the light is in the ultraviolet (UV) and blue end of the visible spectrum (**Figure 1A**). It is most commonly observed as the blue glow in the cooling ponds of spent nuclear fuel.

The charged particles released upon radioactive decay may include electrons (such as β^- particles, Auger electrons and conversion electrons), positrons (β^+), and α -particles. As these particles travel, they lose energy through interactions with the surrounding matter. In the biological context this matter is almost always water. At speeds below the speed of light in water, the randomly oriented water molecules will align with the passing of the charged particle. After the particle passes, these aligned water molecules along this path will relax back to a lowest energy state. In cases when the particle is traveling at super-relativistic phase velocities (i.e. faster than the speed of light in that medium), these polarized molecules relax by releasing energy in the form of visible radiation luminescence.

The threshold speed for CR production is the phase velocity, or speed of light in that medium. The β -particle velocities (v) as a function of energy can be calculated from **Equation 1**.

$$v = c \left(1 - \frac{E_o^2}{(E + E_o)^2} \right)^{1/2} \quad \text{Eq. 1}$$

Here, c is the speed of light in a vacuum, E is the particle energy and E_o is the mass of the β -particle at rest, in the same units as E . The number of Cerenkov photons produced along the β -particle's path can be calculated using the Frank-Tamm formula over a specified region of the light spectrum as **Equation 2** [6].

$$\frac{\partial N}{\partial \lambda} = 2\pi\theta \left(\frac{1}{\lambda_1} - \frac{1}{\lambda_2} \right) \left(1 - \frac{1}{\varphi^2 n^2} \right) \quad \text{for } \varphi n > 1$$

$$\frac{\partial N}{\partial \lambda} = 0 \quad \text{for } \varphi n \leq 1 \quad \text{Eq. 2}$$

Here θ is the fine structure constant (1/137), the λ 's define the spectral range, n is the refractive index of the material and φ is the velocity of the β -particle divided by c . The threshold energy to produce CR can be solved for a β -particle in water (with a refractive index of 1.33), to yield a minimum energy requirement of 263 keV. Many of the β -particles produced by ^{18}F decay possess greater energy than this threshold and therefore produce CR (the ^{18}F endpoint energy is 633 keV and mean is 250 keV). For radionuclides that are studied for biomedical applications (including ^{225}Ac), α -particles are generally not of sufficient energy to produce light directly. However, the CR emissions of daughter isotopes' decay particles have been detected [7]. It should be noted that as this process is refractive index dependent: the E_{\min} is reduced to ≥ 219 keV in tissue (using an approximate refractive index of 1.4) [8]. A direct illustration of this dependence on refractive index is the measurement of light produced in varying media (**Figure 1B**).

At this time, several studies have theoretically and experimentally evaluated nearly all of radioisotopes of interest for CR production [7, 9, 10]. The β -particle energy spectrum and branching ratios for a given radionuclide determines the amount of CR produced photons. Thus, for commonly used radionuclides the number of CR photons produced per disintegration follows the trend of $^{90}\text{Y} > ^{68}\text{Ga} > ^{15}\text{O} > ^{11}\text{C} > ^{124}\text{I} > ^{89}\text{Zr} > ^{18}\text{F} > ^{64}\text{Cu}$. For a particular Cerenkov imaging application, different parameters must be weighed for the choice of radionuclide including the amount of light produced, radiolabeling strategy, half-life of the tracer, and biological implications of the higher energy particles.

Cerenkov luminescence imaging overview

The use of the CR light for direct optical imaging using a CCD was first described by Cho et al., from observations of radioactivity in microfluidic chips [11]. Cerenkov luminescence imaging (CLI), coined in 2009 by Robertson et al., pairs the production of visible light from radiotracers with widely used small animal imaging equipment optimized for preclinical imaging [4]. Optical imaging techniques are workhorses in the biomedical-imaging field that enable interrogation of sub-microscopic to macroscopic features. All optical imaging methods are based on acquisition of photons traveling through and or

Cerenkov luminescence imaging

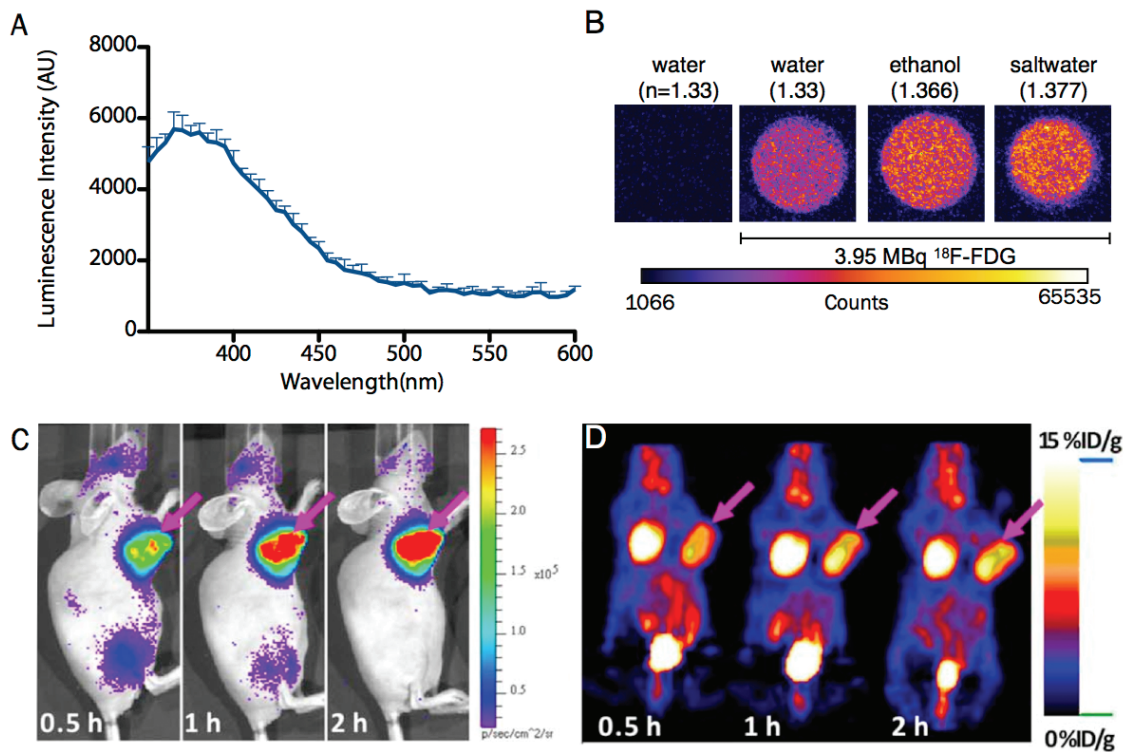


Figure 1. Cerenkov Light and Characteristics. A) Cerenkov radiation (CR) is produced by a charged particle traveling through a dielectric medium faster than the speed of light (in a vacuum) divided by the refractive index of that medium. Relaxation of the molecules in the medium, polarized by the passage of the charged particle, produces visible light weighted towards the higher energy of the spectrum. The profile of the CR is centered at the blue, as shown with ^{68}Ga (18.5 MBq) in 0.1 M HCl diluted in water, using a Molecular Diagnostics M5 spectrophotometer. B) Equal activities of F-18 samples (3.952 MBq, 20 μL) were diluted in 2 mL of water (H_2O , refractive index: $n=1.3359$), ethanol ($\text{C}_2\text{H}_5\text{OH}$, $n=1.366$), saltwater (H_2O and saturating NaCl, $n=1.377$) along with a control sample of water without radionuclide. Samples were read for 20 exposures of 12.5 seconds using Stanford Photonics XR Mega 10 intensified charge-coupled device camera system in a 24 well plate. C) Cerenkov luminescence imaging (CLI) and D) PET imaging of nude mice bearing C6-FLuc tumor injected via tail vein with ^{18}F -FDG at 0.5, 1, 2 h post-injection.

interacting with tissue and cellular components. Among the most widely used techniques for *in vivo* animal imaging are planar and tomographic fluorescence imaging and bioluminescence imaging [12].

Despite their utility, these techniques are largely restricted to preclinical use. Factors that have prevented translation from the bench to the bedside include depth-penetration considerations, regulatory issues and toxicity. Notably, bioluminescent substrates (luciferin and coelenterazine) and enzymes (luciferase) are weakly immunogenic and there are, to the best of our knowledge, only two currently approved fluorescent probes (the non-specific indocyanine green and fluorescein [13-15]). While clinical trials of fluorescent systems continue to progress [16, 17], Cerenkov imaging provides an opportunity

to bridge the optical (preclinical) and nuclear (clinical) gap using approved tracers and therapeutic agents. Therefore, the CR derived from clinical agents (e.g. ^{18}F -FDG) in conjunction with highly sensitive optical imaging equipment may enable facile clinical translation of optical imaging.

Visualizing radiolabeled compounds using optical systems presents several unique advantages but also challenges. Approximate calculations reveal the workflow advantages of CLI for preclinical studies. One to two animals can be scanned in small animal PET equipment, often requiring a scan of 10 minutes or more. In CLI, as many as five animals can be imaged simultaneously, and a white light image of the subjects is also provided for anatomical context. Bioluminescent imaging units are considerably cheaper

than the majority of small animal PET systems, with lower service costs. These combined advantages are particularly relevant for studies that involve many subjects over extended periods of time. Using the radiotracer as an internal light source is also advantageous as it reduces non-specific background signal for the object being imaged. In contrast, fluorescent compounds require an external excitation source. This creates substantial background from surface reflectance, greater tissue autofluorescence as well as in homogenous excitation throughout the volume due to the different absorption properties of tissues.

Radiotracer imaging

Small animal imaging systems that pair a sensitive CCD camera with an animal isolation chamber are widely used for the visualization of bioluminescent signals in genetically modified cells and animals. No significant changes in imaging procedures are required for CLI, other than replacing injection of a bioluminescent substrate with that of a radiotracer. Furthermore, no genetic manipulation is needed to introduce expression of one of the luciferases. The following sections of this review discuss the applications of directly performing CLI on different classes of labeled compounds and agents for varied purposes. These include therapeutic monitoring, reporter gene imaging and optically guided surgery. Following these, a description of some of the inherent and technical challenges to the use of CLI are detailed, along with developing approaches to overcome these issues.

Small molecule radiotracers

The most commonly used PET radiotracer is undoubtedly ¹⁸F-FDG. This modified glucose molecule accumulates at sites of upregulated metabolism, delineating proliferating and inflamed regions. Reported doses of ¹⁸F-FDG imageable with CLI are the same as those used for standard small animal PET studies (approximately several MBq / few hundred μ Ci). Imaging of ¹⁸F-FDG using CLI has been shown to strongly correlate with the absolute concentrations as defined in small animal PET (**Figure 1C** and **1D**) [10, 18].

Beyond detection of a tumor, ¹⁸F-FDG has also been used to monitor disease progression and efficacy of therapy [19]. Robertson et al. have

demonstrated CLI's usefulness in preclinical investigations of drug efficacy, monitoring response to the treatment of lymphoma xenografts with MLN4924, a small molecule inhibitor of NEDD8-activating enzyme. This drug prevents cellular proteasome function and has been shown to induce death in a variety of cancer cell lines [20]. CLI was used to show a statistically significant correlation between total ¹⁸F-FDG uptake (by CLI and PET) and treatment of the SC xenografts.

In a similar approach, Xu et al. utilized both ¹⁸F-FDG and ¹⁸F-FLT in order to investigate the response of H460 (lung) and PC3 (prostate) xenografts to treatment with bevacizumab [21]. This monoclonal antibody targets vascular endothelial growth factor (VEGF) and is FDA approved to treat colorectal, non-small cell, kidney and certain brain tumors. The authors were able to demonstrate a high correlation between PET and CLI for both tracers. Their results further indicate that the efficacy of immunotherapy could be monitored in a high-throughput and low cost manner using CLI.

Small molecule imaging agents for non-oncological applications have also been observed with CLI. The radiolabeled acetylcholinesterase (AChE) inhibitor, 2-[¹⁸F] fluoro-CP-118,954, has been imaged using PET and CLI post-mortem. AChE activity is strongly reduced in post-mortem tissues of Alzheimer's disease patients [22]. The tracer showed high uptake in the striatum on both PET and CLI in healthy mice. This region is rich in AChE activity, demonstrating that this agent may be useful for identification and diagnosis of the neurodegenerative disease.

Finally, these techniques have also been leveraged for non-animal studies. Light produced from fluorine was detected in a microfluidic device [11] and ³²P distribution has been imaged in a plant growth model [23].

CLI and radiotherapy

The ability to image the spatial distribution and concentration of therapeutic radionuclides is of considerable interest to the nuclear medicine community. For some of these isotopes, such as ¹³¹I, imaging is relatively easy given that the decay scheme includes abundant gamma emission for planar scintigraphy and SPECT. How-

ever, other therapeutic nuclides such as ^{90}Y or the α -emitting radionuclides are considerably more difficult to detect. CLI has been utilized in several recent studies in order to achieve imaging in preclinical models. In mice, free $^{90}\text{YCl}_3$ was visualized to rapidly accumulate in the liver and bone [10]. The ^{90}Y radionuclide has also been imaged in an innovative chelate capture scheme. Here, a protein was engineered to bind to a chelate appendage, which can be expressed *in vivo*, or used in a pretargeting approach. Results showed that chelated ^{90}Y cleared from background tissues over several hours, while remaining specifically in tumors expressing the protein [24]. It should be noted that CLI imaging of ^{90}Y may provide an alternate means to efficiently image this nearly pure β -particle emitter, as compared to low count PET and SPECT [25, 26].

^{225}Ac produced considerable luminescence when imaged using small-animal optical imaging equipment [7]. This has spurred interest in the potential to image it *in vivo*, along with other α -emitters such as ^{230}U , ^{212}At and ^{212}Bi . The massive α -particle (relative to a positron) does not itself produce CR [9]. However, many of these radionuclides involve several decay pathways that have significant Cerenkov photon production efficiencies. Modeling of the decay chain and yields has indicated that there is potential benefit for CLI in imaging these radionuclides [27]. However, in some instances the long half-lives of the daughters preclude its being used in a clinical setting.

Reporter gene CLI

Nuclear imaging is a powerful technique to visualize gene expression. It has been used to track cells and/or monitor induction of specific genes [28, 29]. A well-established reporter gene expression strategy is the herpes simplex virus type 1 (HSV1) thymidine kinase (TK) gene. This enzyme (HSV1-tk) phosphorylates and thus traps a number of substrates only within the transfected cells. These substrates include many CR emitting small molecules such as ^{124}I -FIAU, ^{124}I -FEAU and ^{18}F -FHBG. The latter has been used to show that reporter gene expression can be visualized using CLI in a glioma model in mice [30].

Thyroid specific uptake of iodine has long been exploited for radioablation of thyroid neoplasms.

This phenomenon is mediated by the sodium iodide symporter, a surface protein that actively transports I⁻ into thyroid cells [31]. This was first visualized using radioactive iodine for CLI in wildtype mice [10]. Furthering this approach, Jeong et al. have used CLI for visualization of iodide symporter expression in transduced cells. This technique enables high throughput identification of ^{131}I accumulation specifically in implanted cells [32].

Macromolecule radiotracers

The imaging of larger radiolabeled structures such as peptides, antibodies and nanoparticles is also amenable to CLI. For example, a dual-targeting peptide for RGD (binding $\alpha_v\beta_3$ integrin) and bombesin (binding gastrin receptor) was ^{90}Y -labeled. The probe visualized prostate cancer xenografts with high specificity [10]. Likewise, the clinically approved Her2/neu tumor targeted antibody, trastuzumab, can be visualized with this technique. Long lived radionuclides such as ^{89}Zr (78.4 h) [7, 33] and ^{124}I (100.2 h) [23] have been conjugated to the full sized monoclonal antibody to image tumors overexpressing the receptor in mouse models. Longitudinal optical imaging of mice with these compounds can be useful to visualize the clearance time and specific accumulation of these long circulating and specific agents.

Nanoparticle probes have garnered great interest over the past decade for biomedical applications. This is because nanoparticles possess unique and tuneable biological, chemical and physical properties for imaging and therapy. Iron oxide nanoparticles generate negative contrast in magnetic resonance (MR) imaging and have been widely used as a preclinical nanoparticle platform. Labeling of these particles with ^{124}I enabled triple modality imaging of the distribution of the probe for MR, CLI and PET particle trafficking to the lymph nodes [34].

Cerenkov-guided surgery

Molecular specificity using nuclear and optical techniques has tremendous potential in the surgical setting to guide resection using targeted and specifically accumulated agents in diseased tissue. Intraoperative imaging of a radionuclide using CLI is feasible, as demonstrated by Holland et al. using Her2/neu monoclonal antibody targeted to cancerous cells [33].

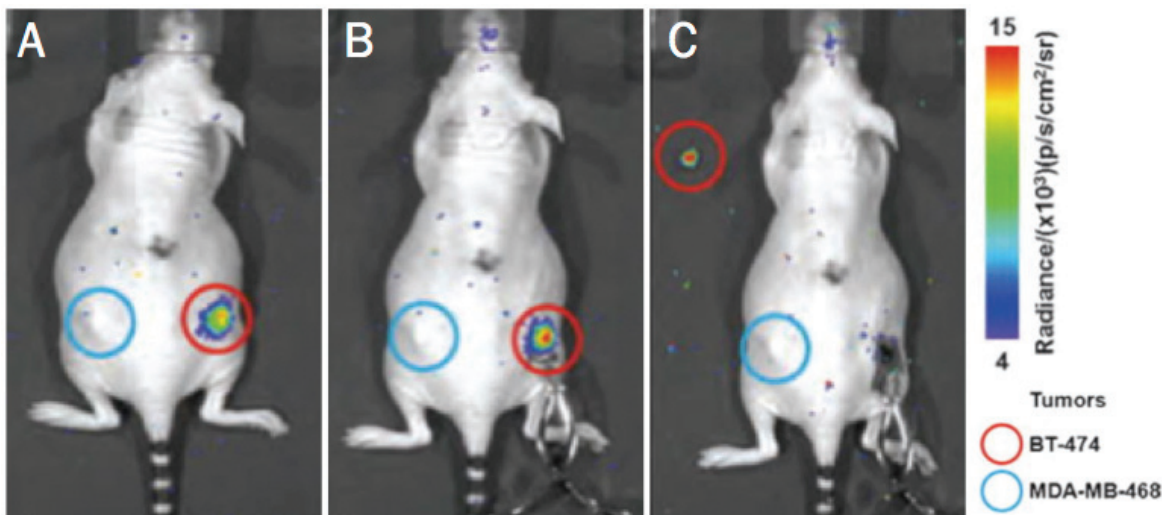


Figure 2. Intraoperative CLI. Intraoperative optical CLI of mouse 4 during surgical resection of the BT-474 (HER2/neu positive) tumor at 144 hours postadministration of ^{89}Zr -DFO-trastuzumab. A) Preoperative optical CLI of mouse 4 prior to surgical incision. B) Intraoperative optical CLI of the exposed tumor immediately prior to resection. Note the increased intensity of the CLI signal owing to reduced attenuation and scattering from removal of the skin. C) Resected tumor (upper left corner) and the exposed incision site showing the complete loss of CLI signal in the exposed region of the mouse. Modified with permission from Holland et al. [33].

The ^{89}Zr -DFO-trastuzumab radiotracer delineated BT-474 (Her2/neu-overexpressing) and MDA-MB-468 (Her2/neu-low expression) tumors. Temporal PET and CLI were used to evaluate the probe's long-term distribution (**Figure 2**). CLI-guided surgery was then performed to resect the BT-474 tumors. Margins of the tumor were clearly visible following removal of skin, and complete removal of the immunotargeted cells was confirmed after surgery.

These results show a tumor region that was visible using optical imaging as late as 144 hours post-injection. This indicates that one injection would be sufficient for pre-, intra-, and post-surgery imaging. In this context, a radiotracer can be used first to determine the exact tumor size and location using pre-surgery PET, followed by definition of accurate tumor margins intraoperatively, and finally to confirm the efficacy of the operation using CLI before closure and post-surgery PET. This application may have significant advantages over current intraoperative radiation detection systems, such as hand-held gamma probes.

Challenges regarding CLI

There are three primary difficulties encountered when using radiotracers as an illumination

source for preclinical imaging. As the CR process is dependent on decay and therefore a reduction in the amount of 'active' material, an important consideration is the half-life of the tracer being used. This is a commonly encountered issue in the nuclear imaging field, but a new limitation for optical studies. While the 110 min half-life of ^{18}F may be suitable for imaging of glucose uptake and accumulation over several hours, it is not suitable for longer experimental investigations that might require days – unless re-injection of ^{18}F -FDG is feasible. However, there are many options in the radiolabel used, and many Cerenkov generating radionuclides possess a long half-life (such as ^{89}Zr ; 78 h).

The second issue concerning practical CLI is that there is relatively little light produced through this process, in comparison to standard bioluminescent and fluorescent strategies. For example, models estimate that the number of visible wavelength photons generated by ^{18}F in a typical ^{18}F -FDG rodent acquisition (using 100 μCi) would be several million photons per second, orders of magnitude lower than that of a typical bioluminescent study [35]. This is partly compensated through the lack of a non-specific background signal. Further, for all but the shortest-lived PET radiotracers, the time of acquisi-

tion can be extended in order to capture greater numbers of photons for imaging purposes. However, the relative paucity of CR requires that other illumination sources be removed. In the diagnostic and operative setting, this presents a problem, as the ambient light required in a normal working environment must be strictly controlled. This suggests that laparoscopic and endoscopic applications might provide an ideal environment for clinical CLI.

A final difficulty involves the spectral character of the light. The blue-weighted Cerenkov is particularly well attenuated by tissues [36]. Thus, there is considerable loss of detectable luminescence as the activity source moves further from the surface of the animal. This presents a problem for deep tissue imaging of larger animals. However, subcutaneous tumors are easily discernible as are organs of high tracer uptake such as the kidneys, spleen, thymus and even the heart in rodent models.

Several approaches are currently being pursued in order to leverage advantages of Cerenkov luminescence imaging to overcome some of these technical challenges, discussed in the following sections.

Cerenkov excitation of fluorophores

UV and blue light are strongly attenuated in tissues. This limitation for deep tissue imaging of Cernekov can possibly be overcome through fluorescent strategies. Here, the aim is to convert the blue-weighted CR to longer wavelengths for enhanced penetration. Cerenkov-induced fluorescent imaging has been demonstrated using a variety of fluorescent probes including small molecules [37] and quantum dot (QD) nanoparticles [38, 39], as seen in (Figure 3A). QD nanoparticles are in many ways ideal fluorescent particles for excitation by a continuous UV-weighted photon source such as CR. QDs absorb light continuously up to their emission wavelength, are photostable and easily conjugated to biologically relevant molecules. Further, they possess fluorescent emission profiles that are characteristically narrow [40, 41]. Together, these features allow the CR to be pushed out of the easily attenuated blue/green region and into the near infrared. It also enables multiplexing as multiple QD excited by the same CR source can be discerned separately using appropriate filters. This contrasts with conven-

tional PET imaging, as all detected coincidence-photon posses the same energy of 511 keV and cannot be separated from each other (Figure 3B and 3C).

Cerenkov for photoactivation therapy

The photoactivation of compounds involves the degradation of a ‘caged’ compound to an active state through a chemical process. These processes can involve biological stimuli (such as enzymatic cleavage) or physical activating events (such as X-ray [42] or UV-light [43]). A commonly used photoactive strategy is the DMNP-luciferin bioluminescence system. Here, the caged substrate (DMNP-luciferin) undergoes photolytic cleavage of a caging-group under 365 nm UV-irradiation. This releases luciferin, the substrate for the luciferase enzyme, a bioluminescent genetic reporter. However, at this low wavelength the activating light penetrates tissues poorly, making external illumination inefficient. Ran et al. activated a caged luciferin substrate through whole-body internal illumination by ¹⁸F-FDG (Figure 3D and 3E). This study was able to demonstrate that ¹⁸F-FDG was efficient at photolytic activation of the DMNP-luciferin using cells *in vitro*, as well as in luciferase expressing cancer cells in a mouse model [44].

The linear accelerators used for external beam irradiation in the clinical setting function by delivering high doses of shaped electron and photon beams. At sufficient energy, these externally impinging electrons are capable of producing CR. Detectable levels of light were generated in a solid phantom and the amount of light produced increased linearly with beam energy (up to 18 MeV), to a fluence rate of approximately 1.1 $\mu\text{W}/\text{cm}^2$ [45]. This light was then used to excite protoporphyrin IX (PpIX), a fluorescent agent that also has therapeutic properties through production of reactive oxygen species. This demonstrates the feasibility of this approach for dual therapy from the beam itself and radiation-induced phototherapy localized to the beam path.

Cerenkov luminescence tomography and dynamic imaging

Several groups have pursued CR as an internal illumination source for tomographic reconstruction (Cerenkov luminescence tomography, CLT). External illumination, e.g. fluorescent tomogra-

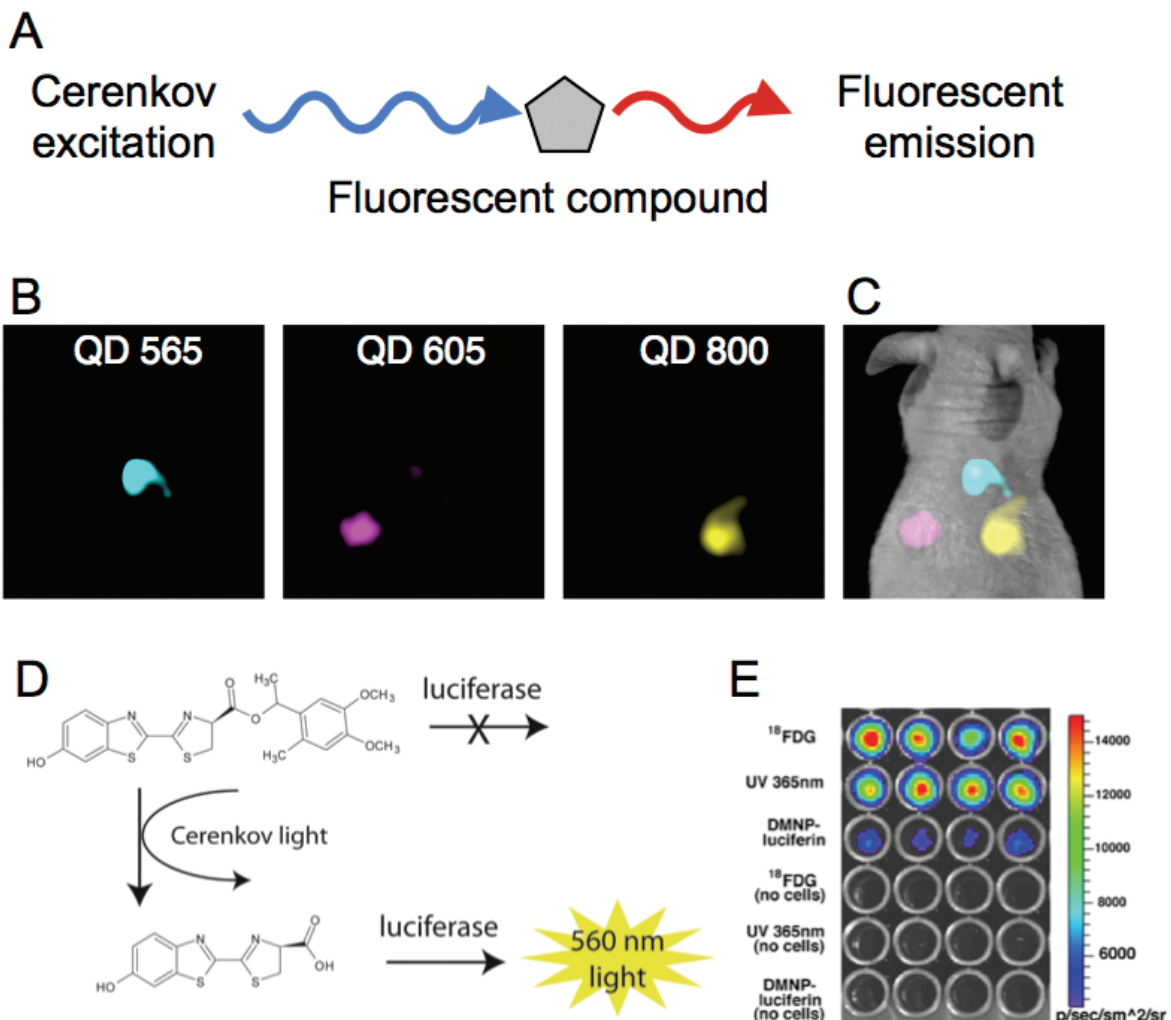


Figure 3. Fluorescent and Photo-activation by CR. To provide for a solution to the depth limitation problem of the blue-weighted CR as well as enable multiplexing in CLI, use of fluorescent compounds has been investigated. A) The principle of secondary Cerenkov-induced fluorescence is to use the radiotracer produced CR in order to excite a fluorescent molecule, protein or nanoparticle. This then emits light shifted to the red which can penetrate deeper tissue. B) A demonstration of the multiplexing capabilities of CLI with fluorophores. Here quantum dots with different emission wavelengths were subcutaneously implanted in the back of a mouse. ¹⁸F-FDG was then intravenously administered and the filter defined emission of each fluorophore was captured and C) combined. The Cerenkov light from a radio-tracer can be used to initiate photodegradation of caged compounds into their active form. D) Scheme of photoactivation of DMNP-luciferin; CR activates the compound enabling the substrate to be consumed by the luciferase enzyme to produce light. E) In vitro assay demonstrating success in using ¹⁸F-FDG to activate the caged substrate and the production of light by luciferase expressing cells.

phy, can undergo several confounding interactions including non-homogeneous excitation, surface reflection and autofluorescence. The internal illumination from radiotracers reduces these issues and has the advantage of being quantitatively validated using established nuclear tomographic techniques.

Several models to solve for the reconstruction

have been pursued [46,47]. Using ¹⁸F-FDG, at imaging times and doses similar to those for PET and CLI, LI et al. demonstrated that fused CLT/CT and PET/CT had high correspondence [48], using a finite element mesh method (**Figure 4**). SPECT techniques have also been used to validate CLT reconstruction, for example with a ¹³¹I source [49]. In a recent development, using an ¹⁸F-FDG tracer, a more sophisticated

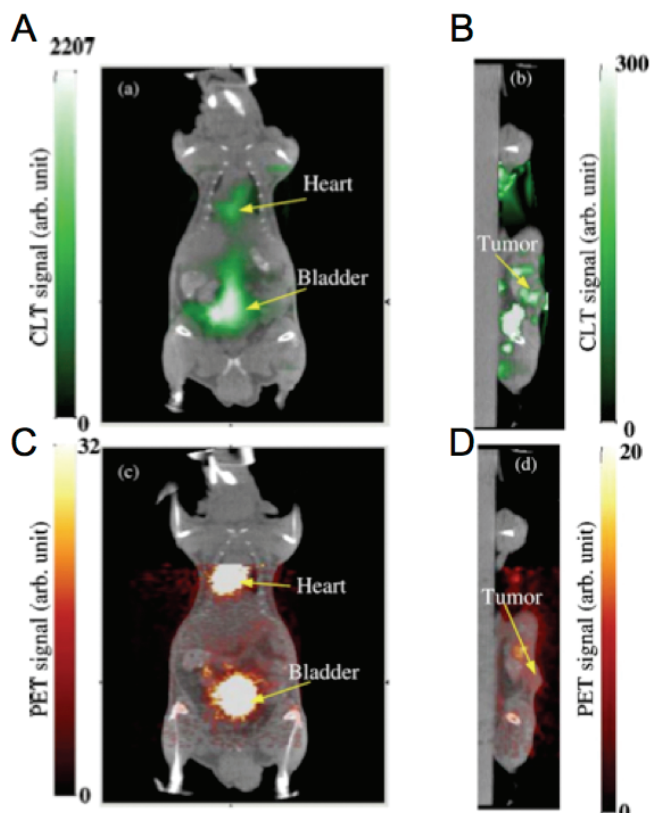


Figure 4. Cerenkov Luminescence Tomography. Reconstructed Cerenkov luminescence tomography images fused with CT images. A) Coronal cross section showing bladder and heart and B) sagittal cross section at tumor. C), D) Corresponding fused PET/CT images.

finite element SP₃ model has been used (to better approximate optical properties of heterogeneous tissues) [50]. Such approaches may be appealing to budget-limited laboratories providing greater reconstruction speed and lower processing requirements.

Addressing the processing time required for this complex model, Zhong et al. have investigated a reconstruction model using L_{1/2} regularization [51]. This approach could be employed in the future for very short half-life radionuclides (e.g. ¹⁵O and ¹¹C, t_{1/2} of 2.04 and 20.4 min, respectively). Additional information may also be derived from the spectral profile of the CR, which passes through several tissue specific absorption domains. Spectrally defined measurements therefore enable three-dimensional reconstruction from a single (not rotated) surface image.

This was demonstrated with ³²P-ATP and readings using bandpass filters for 600, 620, 640 and 660 nm for tomographic whole body distribution in a mouse [46].

A non-tomographic approach to achieve organ (and tumor) delineation is to utilize the dynamic distribution of optical contrast agents [52]. Taking advantage of an electronic camera's ability to acquire frames at high speed, coupled with algorithms for clustering signals (on a per pixel basis) as a function of time, it is possible to anatomic compartmentalization maps. Recently it has been shown that CR produced from ³²P-ATP and ¹⁸F-FDG can be used for such anatomical distinction [53]. This dynamic CLI strategy offers interesting opportunities for compartment modeling of dynamic tracer distribution and automatic demarcation of tumor uptake.

Conclusions

The use of Cerenkov emissions for optical identification of the distribution of radiotracers has generated intense interest in the imaging field. It enables the facile imaging of radiotracer distribution for a variety of useful biomedical and preclinical applications using optical imaging equipment. Applications using common and experimental PET and therapeutic radiopharmaceuticals have the potential to accelerate preclinical nuclear research. As well, the technique may enable facile translation of optical imaging techniques into the clinic with a focus on intraoperative and endoscopic applications.

Acknowledgments

DLJT was supported through the R25T Molecular Imaging Fellowship: Molecular Imaging Training in Oncology (5R25CA096945-07). JG through the Louis V. Gerstner Young Investigator Award and the Starr Cancer Consortium (I4-A427). JH and WAB through the MSKCC-CCNY Partnerships.

Address correspondence to: Dr. Jan Grimm, 1275 York Street, Box 248, Memorial Sloan-Kettering Cancer Center, New York, New York, 10065 E-mail: grimmj@mskcc.org

References

- [1] Cherenkov PA. Visible emission of clean liquids by action of γ radiation. Doklady Akademii Nauk SSSR 1934; 2: 451.
- [2] Wiebe LI, Noujaim AA and Ediss C. Some aspects of the measurement of ^{32}P Cerenkov radiation in water by a liquid scintillation spectrometer. Int J Appl Radiat Isot 1971; 22: 463-467.
- [3] Burch WM. Cerenkov light from ^{32}P as an aid to diagnosis of eye tumours. Nature 1971; 234: 358.
- [4] Robertson R, Germanos MS, Li C, Mitchell GS, Cherry SR and Silva MD. Optical imaging of Cerenkov light generation from positron-emitting radiotracers. Phys Med Biol 2009; 54: N355-365.
- [5] L'Annunziata MF. Radioactivity: introduction and history. Oxford: Elsevier, 2007.
- [6] Frank I, Tamm I. Coherent visible radiation of fast electrons passing through matter. Compt Rend Dokl Akad Mauk SSSR 1937; 14: 109-114.
- [7] Ruggiero A, Holland JP, Lewis JS and Grimm J. Cerenkov luminescence imaging of medical isotopes. J Nucl Med 2010; 51: 1123-1130.
- [8] Beattie BJ, Thorek DLJ, Schmidlein CR, Pentlow KS, Humm JL and Helscher AH. Quantitative modeling of Cerenkov light production efficiency from medical radionuclides. PLoS One 2012; 7: e31402.
- [9] Beattie BJ TD, Schmidlein CR, Pentlow KS, Humm JL, Helscher AH. Quantitative modeling of Cerenkov light production efficiency from medical radionuclides. PLoS One 2012; 7: e31402.
- [10] Liu H, Ren G, Miao Z, Zhang X, Tang X, Han P, Gambhir SS and Cheng Z. Molecular Optical Imaging with Radioactive Probes. PLoS One 2010; 5: e9470.
- [11] Cho JS, Taschereau R, Olma S, Liu K, Chen YC, Shen CK, van Dam RM, Chatziloannou AF. Cerenkov radiation imaging as a method for quantitative measurements of beta particles in a microfluidic chip. Phys Med Biol 2009; 54: 6757.
- [12] Massoud TF, Gambhir SS. Molecular imaging in living subjects: seeing fundamental biological processes in a new light. Genes Dev 2003; 17: 545-580.
- [13] Hochheimer BF. Angiography of the retina with indocyanine green. Arch Ophthalmol 1971; 86: 564-565.
- [14] Flower RW. Injection technique for indocyanine green and sodium fluorescein dye angiography of the eye. Invest Ophthalmol 1973; 12: 881-895.
- [15] Friberg TR, Rehkopf PG, Warnick JW and Eller AW. Use of directly acquired digital fundus and fluorescein angiographic images in the diagnosis of retinal disease. Retina 1987; 7: 246-251.
- [16] Bremer C, Ntziachristos V and Weissleder R. Optical-based molecular imaging: contrast agents and potential medical applications. Eur Radiol 2003; 13: 231-243.
- [17] Choy G, Choyke P and Libutti SK. Current advances in molecular imaging: noninvasive *in vivo* bioluminescent and fluorescent optical imaging in cancer research. Mol Imaging 2003; 2: 303-312.
- [18] Boschi F, Calderan L, D'Ambrosio D, Marengo M, Fenzi A, Calandrino R, Sbarbati A and Spinelli AE. In vivo ^{18}F -FDG tumour uptake measurements in small animals using Cerenkov radiation. Eur J Nucl Med Mol Imaging 2011; 38: 120-127.
- [19] Robertson R, Germanos MS, Manfredi MG, Smith PG and Silva MD. Multimodal Imaging with ^{18}F -FDG PET and Cerenkov Luminescence Imaging After MLN4924 Treatment in a Human Lymphoma Xenograft Model. J Nucl Med 2011; 52: 1764-1769.
- [20] Deshaies RJ. Drug discovery: Fresh target for cancer therapy. Nature 2009; 458: 709-710.
- [21] Xu Y, Chang E, Liu H, Jiang H, Gambhir SS and Cheng Z. Proof-of-Concept Study of Monitoring Cancer Drug Therapy with Cerenkov Luminescence Imaging. J Nucl Med 2012; 53: 312-317.
- [22] Frey KA, Minoshima S and Kuhl DE. Neurochemical imaging of Alzheimer's disease and other degenerative dementias. Q J Nucl Med 1998; 42: 166-178.
- [23] Park JC, Il An G, Park SI, Oh J, Kim HJ, Su Ha Y, Wang EK, Min Kim K, Kim JY, Lee J, Welch MJ and Yoo J. Luminescence imaging using radionuclides: a potential application in molecular imaging. Nucl Med Biol 2011; 38: 321-329.
- [24] Aweda TA, Eskandari V, Kukis DL, Boucher DL, Marquez BV, Beck HE, Mitchell GS, Cherry SR and Meares CF. New Covalent Capture Probes for Imaging and Therapy, Based on a Combination of Binding Affinity and Disulfide Bond Formation. Bioconju Chem 2011; 22: 1479-1483.
- [25] Gates VL, Esmail AAH, Marshall K, Spies S and Salem R. Internal Pair Production of ^{90}Y Permits Hepatic Localization of Microspheres Using Routine PET: Proof of Concept. J Nucl Med 2011; 52: 72-76.
- [26] Selwyn RG, Nickles RJ, Thomadsen BR, DeWerd LA and Micka JA. A new internal pair production branching ratio of ^{90}Y : the development of a non-destructive assay for ^{90}Y and ^{90}Sr . Appl Radiat Isot 2007; 65: 318-327.
- [27] Ackerman NL, Graves EE. The potential for Cerenkov luminescence imaging of alpha-emitting radionuclides. Phys Med Biol 2012; 57: 771.
- [28] Kircher MF, Gambhir SS and Grimm J. Noninvasive cell-tracking methods. Nat Rev Clin Oncol 2011; 8: 677-688.
- [29] Ruggiero A, Thorek DL, Guenoun J, Krestin GP and Bernsen MR. Cell tracking in cardiac repair: what to image and how to image. Eur Radiol

Cerenkov luminescence imaging

- 2012; 22: 189-204.
- [30] Cheng Z, Liu HG, Ren G, Liu SL, Zhang XF, Chen LX and Han PZ. Optical imaging of reporter gene expression using a positron-emission-tomography probe. *J Biomed Opt* 2010; 15: 060505.
- [31] Dohán O, De la Vieja A, Paroder V, Riedel C, Artani M, Reed M, Ginter CS and Carrasco N. The Sodium/Iodide Symporter (NIS): Characterization, Regulation, and Medical Significance. *Endocr Rev* 2003; 24: 48-77.
- [32] Jeong SY, Hwang MH, Kim JE, Kang S, Park JC, Yoo J, Ha JH, Lee SW, Ahn BC and Lee J. Combined Cerenkov luminescence and nuclear imaging of radioiodine in the thyroid gland and thyroid cancer cells expressing sodium iodide symporter: Initial feasibility study. *Endocr J* 2011; 58: 575-583.
- [33] Holland JP, Norman G, Ruggiero A, Lewis JS and Grimm J. Intraoperative imaging of positron emission tomographic radiotracers using cerenkov luminescence emissions. *Mol Imaging* 2011; 10: 1-3.
- [34] Park JC, Yu MK, An GI, Park S-I, Oh J, Kim HJ, Kim JH, Wang EK, Hong IH, Ha YS, Choi TH, Jeong KS, Chang Y, Welch MJ, Jon S and Yoo J. Facile Preparation of a Hybrid Nanoprobe for Triple-Modality Optical/PET/MR Imaging. *Small* 2010; 6: 2863-2868.
- [35] Mitchell GS. In vivo Cerenkov luminescence imaging: a new tool for molecular imaging. *Phil Trans R Soc A* 2011; 369: 4605-4619.
- [36] Spinelli AE, D'Ambrosio D, Calderano L, Marengo M, Sbarbat A and Boschi F. Cerenkov radiation allows in vivo optical imaging of positron emitting radiotracers. *Phys Med Biol* 2010; 55: 483-495.
- [37] Lewis MA, Kodibagkar VD, Oz OK and Mason RP. On the potential for molecular imaging with Cerenkov luminescence. *Opt Lett* 2010; 35: 3889-3891.
- [38] Dothager RS, Goiffon RJ, Jackson E, Harpstite S and Piwnica-Worms D. Cerenkov Radiation Energy Transfer (CRET) Imaging: A Novel Method for Optical Imaging of PET Isotopes in Biological Systems. *PLoS One* 2010; 5: e13300.
- [39] Liu H, Zhang X, Xing B, Han P, Gambhir SS and Cheng Z. Radiation-Luminescence-Excited Quantum Dots for in vivo Multiplexed Optical Imaging. *Small* 2010; 6: 1087-1091.
- [40] Bruchez M, Moronne M, Gin P, Weiss S and Alivisatos AP. Semiconductor Nanocrystals as Fluorescent Biological Labels. *Science* 1998; 281: 2013-2016.
- [41] Chan WCW, Nie S. Quantum Dot Bioconjugates for Ultrasensitive Nonisotopic Detection. *Science* 1998; 281: 2016-2018.
- [42] Petit M, Bort G, Doan BT, Sicard C, Ogden D, Scherman D, Ferroud C and Dalko PI. X-ray Photolysis to Release Ligands from Caged Reagents by an Intramolecular Antenna Sensitive to Magnetic Resonance Imaging. *Angew Chem Int Ed Engl* 2011; 50: 9708-9711.
- [43] Korkotian E, Oron D, Silberberg Y and Segal M. Confocal microscopic imaging of fast UV-laser photolysis of caged compounds. *J Neurosci Methods* 2004; 133: 153-159.
- [44] Ran C, Zhang Z, Hooker J and Moore A. In Vivo Photoactivation Without "Light": Use of Cerenkov Radiation to Overcome the Penetration Limit of Light. *Mol Imaging Biol* 2011; [Epub ahead of print].
- [45] Axelsson J. Cerenkov emission induced by external beam radiation stimulates molecular fluorescence. *Med Phys* 2011; 38: 4127.
- [46] Spinelli AE, Kuo C, Rice BW, Calandrino R, Marzolla P, Sbarbat A and Boschi F. Multispectral Cerenkov luminescence tomography for small animal optical imaging. *Opt Express* 2011; 19: 12605-12618.
- [47] Zhong J, Qin C, Yang X, Zhu S, Zhang X and Tian J. Cerenkov Luminescence Tomography for In Vivo Radiopharmaceutical Imaging. *Int J Biomed Imaging* 2011; 2011: 641618.
- [48] Li CQ, Mitchell GS and Cherry SR. Cerenkov luminescence tomography for small-animal imaging. *Opt Lett* 2010; 35: 1109-1111.
- [49] Hu Z, Liang J, Yang W, Fan W, Li C, Ma X, Chen X, Ma X, Li X, Qu X, Wang J, Cao F and Tian J. Experimental Cerenkov luminescence tomography of the mouse model with SPECT imaging validation. *Opt Express* 2010; 18: 24441-24450.
- [50] Zhong J, Tian J, Yang X and Qin C. Whole-Body Cerenkov Luminescence Tomography with the Finite Element SP3 Method. *Ann Biomed Eng* 2011; 39: 1728-1735.
- [51] Zhong J, Qin C, Yang X, Chen Z, Yang X and Tian J. Fast-Specific Tomography Imaging via Cerenkov Emission. *Mol Imaging Biol* 2011; [Epub ahead of print].
- [52] Hillman EMC, Moore A. All-optical anatomical co-registration for molecular imaging of small animals using dynamic contrast. *Nat Photon* 2007; 1: 526-530.
- [53] Spinelli AE, Boschi F. Unsupervised analysis of small animal dynamic Cerenkov luminescence imaging. *J Biomed Opt* 2011; 16: 120507-120503.